International Journal of Advanced Engineering and Technology Research
ISSN: 3106-8677 (Print), ISSN: 3106-8685 (Online) | Vol. 1, No. 3, 2026

Dual-Motor Synchronous Control Method for Mining Electric Locomotives Based on Multi-Strategy Improved Cross-Coupling

Gaoming Feng *, Yujie Zhang

Henan Polytechnic University, Jiaozuo Henan 454000, China

Abstract: To address the speed synchronization error in the dual permanent magnet synchronous motor (PMSM) control system for mining electric locomotives, this paper proposes an improved synchronous control method based on multi-strategy optimized cross-coupling control. The synchronization error characteristics are analyzed, and the dual-motor system model is established under the cross-coupling structure. A double exponential decay prescribed performance function is designed to achieve fast error convergence combined with Lyapunov stability analysis. Meanwhile, a disturbance observer is constructed to estimate and compensate for the lumped disturbance, thus improving control accuracy. Furthermore, a non-singular integral terminal sliding mode controller is designed to satisfy error constraints and enhance system stability. Experimental results demonstrate that compared with traditional cross-coupling control, the proposed method shortens the settling time by 25% and restricts the overshoot within 20 r/min under no-load conditions. Under sudden load impact, the speed recovery time is reduced by 28%, and the synchronization error is significantly reduced.

Keywords: Mining electric locomotive, permanent magnet synchronous motor (PMSM), dual-motor synchronous control, multi-strategy improved cross-coupling.

1. Introduction

From this section, input the body of your manuscript according to the constitution that you had. For detailed information for authors, please refer to [1].

As a core component of the global energy structure, the coal industry confronts unprecedented challenges and opportunities amid the ongoing energy transition [1-5]. Mining electric locomotives, critical for long-distance transportation in mine roadways and on the ground [6], rely heavily on operational stability to ensure transportation efficiency and workplace safety. The dual permanent magnet synchronous motor (PMSM) drive system has become the preferred choice for mining electric locomotives due to its high efficiency, energy-saving benefits, and superior dynamic performance [7, 8]. However, synchronous control of dual motors is prone to synchronization errors under complex underground conditions, such as sudden load changes and parameter perturbations. Excessive synchronization errors not only accelerate transmission component wear and increase energy consumption but also induce power system degradation and even equipment failures, posing severe threats to underground operational safety. Thus, suppressing synchronization errors within a preset precision range is essential for the safe and long-term operation of dual-motor systems in mining electric locomotives [9].

The synchronization performance of dual-motor systems is predominantly determined by control algorithms and structures. Current mainstream control structures include master command control [10], master-slave control [11], cross-coupling control [12-14], and deviation coupling control [15]. Among them, cross-coupling systems are commonly employed in dual-motor synchronous control [16-19]. To enhance synchronization accuracy and anti-disturbance capability, modern control algorithms such as sliding mode control [20, 21], fuzzy control [22, 23], and neural network control [24] have been widely integrated into system design.

Nevertheless, existing approaches exhibit inherent limitations in complex mining scenarios. For instance, the neural network-based parallel control strategy proposed in [25] relies heavily on the quantity and quality of training samples, leading to suboptimal performance under complex conditions. The multi-motor coordination scheme for road-rail dual-purpose vehicles [26] focuses on ground operations and requires further refinement for underground applications. While the fuzzy active disturbance rejection deviation coupling control in [27] improves synchronization for fixed belt conveyors, it lacks robustness against dynamic vibrations and sudden loads of mobile locomotives, as well as real-time adaptability for dual-motor dynamic coordination. For cross-coupling control, strategies in [28-30] have demonstrated effectiveness in industrial high-power transmission or servo systems but fail to cope with uncertain external disturbances in underground mining environments, limiting their synchronization performance.

To address these issues, this letter proposes a multi-strategy improved cross-coupling controller. Firstly, a dual-motor system model is established using a cross-coupling structure based on the analysis of speed synchronization errors. Secondly, a double exponential decay-type prescribed performance function is designed with the Lyapunov function to achieve rapid error convergence. Thirdly, a disturbance observer is constructed to estimate lumped disturbances for feedforward compensation, enhancing error compensation accuracy. Finally, a sliding mode controller is developed using a non-singular integral terminal sliding mode surface and terminal sliding mode reaching law to meet error constraints and improve system stability. Simulation results validate the feasibility and superior performance of the proposed control structure and algorithm.

2. Materials and Methods

This paper adopts the cross-coupling control method to realize the speed synchronous control of dual PMSMs. Motor 1 and Motor 2 adopt the same control strategy of Field Oriented Control (FOC).

The PMSM based on FOC consists of three parts: speed loop, current loop and Pulse Width Modulation (PWM). he control structure diagram is shown in Fig.1. The speed loop is regulated by a specific controller, the d-axis current reference command is zero, and the q-axis current reference command is the output of the speed loop. The PWM part adopts the Space Vector Pulse Width Modulation (SVPWM) control algorithm with good dynamic performance and anti-disturbance capability, which is more suitable for digital control systems. The actual operating speeds of Motor 1 and Motor 2 are ω_1 and ω_2, respectively. The difference between ω_1 and ω_2 is taken as the output speed compensation signal, which is compensated to the input ends of the speed loops of Motor 1 and Motor 2 respectively, so as realize the synchronous operation of the two motors.

To simplify the analysis, the following assumptions are made in the process of PMSM modeling and analysis:

(1) Ignore the harmonic effect, the rotor permanent magnet magnetic field is distributed as a sine wave in the air gap space, and the induced electromotive force in the stator armature winding is a sine wave.

(2) Ignore the saturation of the stator core, regard the magnetic circuit as linear, and the inductance parameters are constant.

(3) Neglect the core hysteresis and eddy current losses.

(4) Do not consider the influence of frequency and temperature changes on motor parameters.

(5) There is no damp wind on the rotor, and the permanent magnet has no damping effect.

Under the above assumptions, the voltage equation of PMSM established in the d-q axis is:

$$\begin{cases} u_{\mathrm{d}} = Ri_{\mathrm{d}} + \dfrac{\mathrm{d}}{\mathrm{dt}}\psi_{\mathrm{d}} - \omega_{\mathrm{e}}\psi_{\mathrm{q}} \\ u_{\mathrm{q}} = Ri_{\mathrm{q}} + \dfrac{\mathrm{d}}{\mathrm{dt}}\psi_{\mathrm{q}} - \omega_{\mathrm{e}}\psi_{\mathrm{d}} \end{cases} \tag{1}$$

Where, u_d and u_q are the stator voltage components of the d-q axis respectively; i_d and i_q are the d-q axis components of the stator current respectively; R is the stator resistance of the motor; ω_e is the electrical angular velocity of the motor; ψ_d and ψ_q are the flux linkage components of the motor.

The electromagnetic torque of PMSM in the d-q axis coordinate system can be ex-pressed as:

$$T_e = \frac{3}{2} p\Phi_f i_q \tag{2}$$

Where, Te is the electromagnetic torque of the PMSM; p is the pole pair number of the motor.

The motion equation of PMSM is:

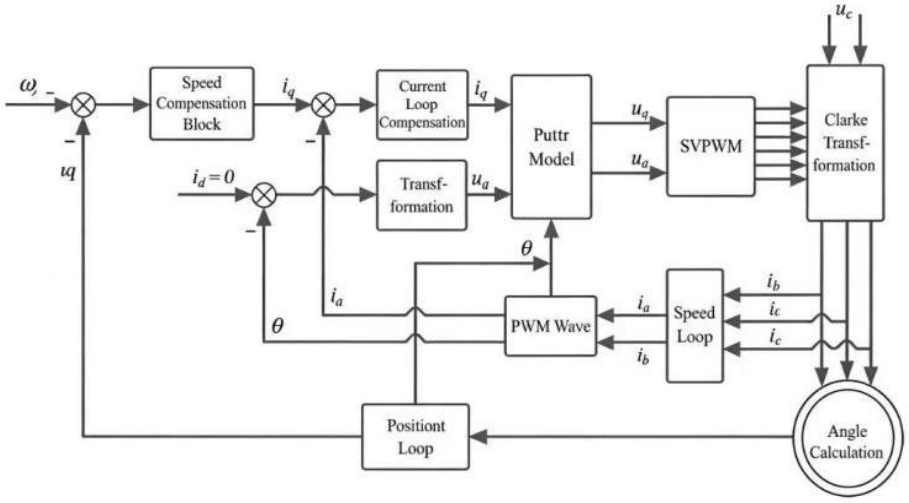

Figure 1. Vector control structure diagram of PMSM with i_d=0

$$J\frac{d\omega_i}{dt} + B\omega_i = T_e + f_i (i = 1, 2) \tag{3}$$

Where, ω_i is the mechanical angular velocity of motor i, J is the moment of inertia of the motor, B is the friction coefficient of the motor, f_i is the lumped disturbance of motor i (including load disturbance and parameter error), and T_L is the load torque.

To simplify the operation, the formula is rewritten as:

$$\dot{\omega}_i = \frac{1.5p\Phi_f i_q}{J} - \frac{B\omega_i}{J} + f_i = b_i i_q + d_i \tag{4}$$

Where, b_i=1.5pf_i/J, d_i=f_i-Bω_i/J

2.1. Design of Prescribed Performance Function

Ai-ming at the dynamic constraint of dual PMSM synchronization error and to break the limitation of delayed convergence boundary of traditional prescribed performance functions, a double exponential decay-type time-varying prescribed performance constraint function is designed:

$$\varepsilon(t) = \begin{cases} (\varepsilon_0 - \varepsilon_T)\alpha^{-\frac{t}{T-t}} + \varepsilon_T, 0 \le t < T \\ \varepsilon_T, t \ge T \end{cases} \tag{5}$$

Where α>1 is the convergence rate adjustment parameter; ε_0 and ε_T are the initial and steady-state values of the function, satisfying ε_0>ε_T>0.

The synchronization error $e_s(t)$=ω_1-ω_2 must satisfy:

$$-\varepsilon(t) < e_s(t) < \varepsilon(t) \tag{6}$$

The tracking error e_ω can converge to $\Omega=\{e_\omega \in R \mid |e_\omega(t)| \le \varepsilon_T\}$ within preset time T, and T, εT can be set according to actual working conditions. The prescribed performance function must be positive definite and strictly monotonically decreasing in the time domain and satisfy $|e_\omega(0)| \le \varepsilon(0)$.

To realize the constraint of Formula (6), an auxiliary function is defined:

$$\kappa = \varepsilon^2(t) - e_s^2(t) \tag{7}$$

Based on this, $\delta(t)$ is constructed to map κ to the interval (0, 1]:

$$\delta(\kappa) = \begin{cases} 1, \eta < \kappa \\ 1 - (\dfrac{\kappa}{\eta} - 1)^{2n}, 0 < \kappa \le \eta \\ 1, \kappa \le 0 \end{cases} \tag{8}$$

Where: η is the maximum safe distance, $\eta \in \left(0 \quad \varepsilon_T^2\right]$, $n \in N^*$, and N^* is a positive integer.

The synchronization error is transformed as:

$$\vartheta = \frac{e_s}{\delta(\kappa)} \tag{9}$$

The boundedness of the transformed error ϑ ensures $e_\omega(t) < \varepsilon(t)$, and $\vartheta = 0 \Leftrightarrow e_\omega = 0$; when $\kappa > \eta$, $\vartheta = e_\omega$; when $e_\omega(t) \to \varepsilon(t)$, $\vartheta \to \infty$, forcing $e_\omega(t)$ to be within the preset boundary.

The derivative of the transformed error is:

$$\dot{\vartheta} = \lambda \dot{e}_s + \hbar \tag{10}$$

Where:

$$\hbar = \begin{cases} 0, \eta < \kappa \\ \dfrac{4n\varepsilon\dot{\varepsilon}e_s}{\eta\delta^2}\left(\dfrac{\kappa}{\eta} - 1\right)^{2n-1}, 0 < \kappa \le \eta \\ 0, \kappa \le 0 \end{cases};$$

$$\lambda = \begin{cases} 1, \eta < \kappa \\ \dfrac{1}{\delta} - \dfrac{4ne_s^2}{\eta\delta^2}\left(\dfrac{\kappa}{\eta} - 1\right)^{2n-1}, 0 < \kappa \le \eta \\ 1, \kappa \le 0 \end{cases},$$

And satisfy $\lambda > 0$.

2.2. Design of Disturbance Observer

To improve synchronization control precision, weaken the influence of uncertain factors on system stability, and suppress the estimation peak problem, a time-varying disturbance observer is designed to estimate the lumped disturbance d(t) in real time for feedforward compensation.

Assume that d(t) and its first derivative are bounded, i.e, $|d(t)| < D$, D is a positive unknown constant, and $d(t) \ne 0$.

Define the speed estimation error as $\hat{e}_\omega = \hat{\omega}_1 - \hat{\omega}_2$ ($\hat{\omega}$ is the estimated value of mechanical angular velocity ω), the time-varying disturbance observer is:

$$\begin{cases} \dot{\hat{\omega}}_i = bi_{qi} + \hat{d}_i + L_{1i}(t) sig^{r_1}(\tilde{e}_{\omega i}) \\ \dot{\hat{d}}_i = L_{2i}(t) sig^{r_2}(\tilde{e}_{\omega i}) \end{cases} \tag{11}$$

Where, $\hat{\omega}$ is the estimated value of angular velocity, $\hat{d}_i$ is the estimated value of disturbance, $e_{\omega i} = \omega_i - \hat{\omega}_i$ is the angular velocity estimation error, $sig^r(x) = |x|^r sign(x)$, $L_{1i}(t)$ and $L_{2i}(t)$ are time-varying gains, defined as: $L_{ji}(t) = (l_{ji}0 - l_{ji})e^{-\mu_j t} + l_{ji}$, j=1, 2;

$l_{ji}0$ is the initial gain, l_{ji} is the steady-state gain, and μj is the attenuation coefficient.

2.3. Design of Sliding Mode Controller

Define the non-singular integral terminal sliding mode surface:

$$s_i = \vartheta_i + \beta_i \int_0^t |\vartheta_i|^{\lambda_i} sign(\vartheta_i) d\tau + k_c \vartheta_s \tag{12}$$

Where: $\beta_i > 0$, $0 < \lambda_i < 1$ are the adjustable parameters of the sliding mode surface. Kc is the cross-coupling coefficient to enhance synchronization performance.

Derive the sliding mode surface:

$$\begin{aligned} \dot{s}_i &= \dot{\vartheta}_i + \beta_i |\vartheta_i| sign(\vartheta_i) d\tau + k_c \dot{\vartheta}_s \\ &= \lambda_i \dot{e}_s + \hbar + \beta |\vartheta|^{\lambda} sign(\vartheta) \end{aligned} \tag{13}$$

Select the terminal sliding mode reaching law:

$$\dot{s}_i = -k_{1i} |s_i|^{r_i} sign(s_i) - k_{2i} s_i \tag{14}$$

When deducing the control input i_{qi}^* according to the above formulas, it is necessary to include the disturbance observer compensation term $\hat{d}_i$ and the synchronization error feedback:

$$\begin{aligned} i_{qi}^* = \frac{1}{b_i \lambda_i} \Big[& \lambda_i \dot{\omega}_i + \hbar_i + \beta_i |\vartheta_i|^{\lambda_i} sign(\vartheta_i) \\ & + k_{1i} |s_i|^{r_i} sign(s_i) + k_{2i} s_i - \lambda_i \hat{d}_i - k_c \dot{\vartheta}_s \Big] \end{aligned} \tag{15}$$

2.4. Stability Analysis

To prove that the prescribed performance sliding mode controller can ensure that the dual-motor synchronization error converges to 0 under the prescribed performance index, the stability of the system needs to be analyzed. We select the Lyapunov function V as:

$$V = \frac{1}{2} s^2 \tag{16}$$

Derive V with respect to time t:

$$\dot{V} = s\dot{s} \tag{17}$$

The derivative expression of the sliding mode surface and the terminal sliding mode reaching law have been obtained above. Substitute the above Formula (14) into it, we get:

$$\dot{V} = s\left(-k_1 |s|^r sign(s) - k_2 s\right) \tag{18}$$

According to the function property, $s|s|^r sign(s) = |s|^{r+1}$, then:

$$\dot{V} = -k_1 |s|^{r+1} - k_2 s^2 \tag{19}$$

Since $k_1>0$, $k_2>0$ and r+1>0, for any non-zero s, $|s|^{r+1}>0$ and $s^2>0$. Therefore:

When s≠0,

$$\dot{V} = -k_1 |s|^{r+1} - k_2 s^2 < 0$$

When s=0,

$$\dot{V} = 0$$

According to the Lyapunov stability theory, if there exists a positive definite Lyapunov function V and its derivative $\dot{V}$ is negative semi-definite, the system is stable. Moreover, since $\dot{V}$ is strictly less than zero (except for s=0), the system is asymptotically stable.

To further prove the finite-time convergence of the system, consider the following lemma:

Lemma: For a continuous-time system $\dot{x} = f(x)$, if there exists a continuously differentiable positive definite function V(x) and positive constants a, b and 0<γ<1, such that $\dot{V}(x) \le -aV\gamma(x) - bV(x)$ is satisfied for all x≠0, then the system state x will converge to zero within a finite time T_0, where T_0 satisfies:

$$T_0 \le \frac{1}{b(1-\gamma)} \ln\left(\frac{bV^{1-\gamma}(x(0))+a}{a}\right) \tag{20}$$

For the system, because $V = \frac{1}{2}s^2$, then $|s| = (2V)^{\frac{1}{2}}$, so:

$$\dot{V} = -k_1 (2V)^{\frac{r+1}{2}} - 2k_2 V \tag{21}$$

Let $a = k_1 2^{\frac{r+1}{2}}$, b=2k2, $\gamma = \frac{r+1}{2}$. Since 0<r<1, then 0<γ<1.

Then,

$$\dot{V} \le -aV^{\gamma}(x) - bV(x) \tag{22}$$

According to the above lemma, the sliding mode surface s will converge to zero within a finite time T_0.

3. Simulation Verification of the New Motor Synchronous System

To verify the effectiveness of the cross-coupling controller designed in this paper, modeling and simulation analysis are carried out by using MATLAB/Simulink.

Table 1. PMSM Simulation Parameters

Parameter (Unit)	Motor 1	Motor 2
Rated speed (r·min⁻¹)	1500	1500
Rs (Ω)	2.875	2.700
$L_d = L_q$ (H)	0.0085	0.0080
Ψ_f (Wb)	0.175	0.170
J(kg·m2)	0.008	0.008
B (N·m·s)	0.003	0.003
Pole pair number P_n	2	2

Dual motors for traction of mining electric locomotives generally use two motors with consistent parameters, but in practice, there are slight errors in motor parameters. The parameters of the two PMSMs in the simulation are shown in Table 1. In the simulation model of the new dual-motor synchronous control system, the parameters of the prescribed performance sliding mode cross-coupling controller are: β=10, λ=0.5, k1=5, k2=2, l0=10, l=100, μ=1, kc=2, η=0.6, n=1.

3.1. No-Load Speed Regulation Condition Simulation

This section verifies the performance comparison between the proposed cross-coupling control method based on multi-strategy improvements and the traditional cross-coupling control under the condition of speed up and down. The starting speed is set to 800 r/min; the given speed value is increased to 1000 r/min at 0.1 s; the given speed value is increased to 1200 r/min at 0.2 s; the given speed value is decreased to 800 r/min at 0.3 s. During the simulation test, no load disturbance is added to the two PMSMs during operation. Fig. 2 shows the no-load speed response curves under the traditional method and the cross-coupling control respectively, and Fig. 3 shows the synchronization error, which represents the output speed difference between the two motors.

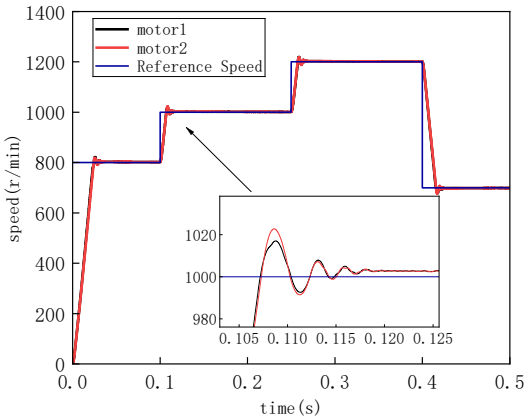

a) Output Speed

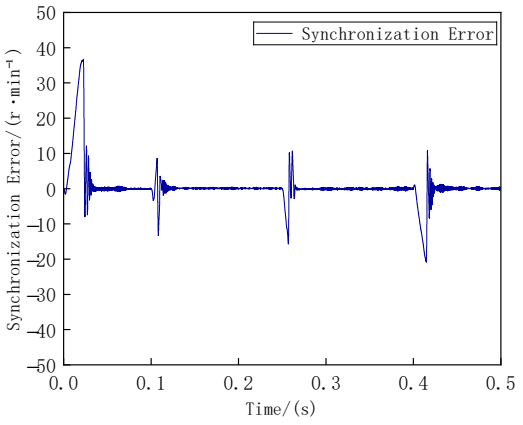

b) Synchronization Error

Figure 2. No-load speed regulation experiment of traditional method

It can be seen from Fig. 2 that under the traditional cross-coupling control method, the overshoot of the dual-motor speed in the steady-state process is 2.5%, there are obvious oscillations and many oscillation times in the transient process, the speed adjustment time is 0.02 s, and the synchronization error fluctuates greatly.

It can be seen from Fig. 3 that under the multi-strategy improved cross-coupling control, the dual motors can track the given speed quickly and accurately, the adjustment time is shortened to 0.015 s, the overshoot is controlled within 2%, there is no oscillation in the transient process, and the speed

tracking consistency is stronger.

In summary, under normal operating conditions, compared with the traditional cross-coupling control, the multi-strategy improved cross-coupling control method reduces the adjustment time by 25% under the no-load speed regulation condition, controls the overshoot more accurately, has better transient stability, and achieves a better control effect on the synchronization error.

3.2. Sudden Load Condition Simulation

This section verifies the performance This section verifies the performance comparison between the proposed method and the cross-coupling control under the sudden load condition. The motor starts at 1200 r/min, and different load disturbances are suddenly applied to the two motors during stable operation. Among them, a load of 10 N·m is suddenly applied to Motor 1 at 0.2 s, and a load of 10 N·m is suddenly applied to Motor 2 at 0.4 s. Fig.4 and Fig. 5 show the load disturbance speed response curves under the traditional method and the cross-coupling control respectively.

It can be seen from Fig.4 that under the traditional cross-coupling control, the dynamic drop of the dual-motor speed reaches 55 r/min

When the load is suddenly applied, the minimum speed change is 5 r/min, the time required for the speed to recover to a stable state is about 0.07 s, the synchronization error increases significantly under load disturbance, and the system has weak anti-disturbance capability.

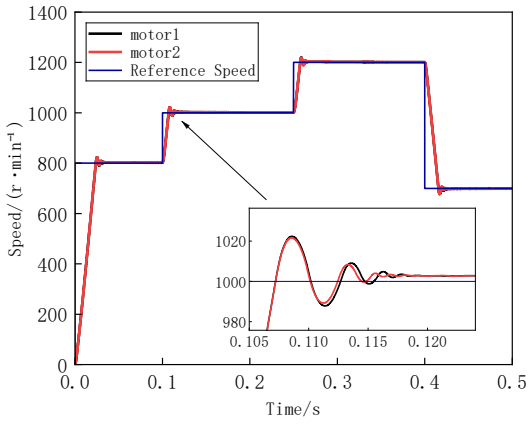

a) Output Speed

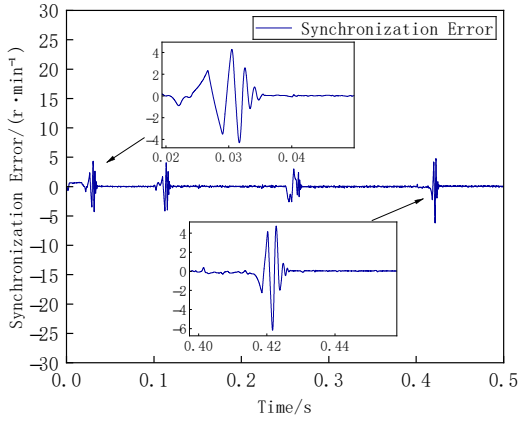

b) Synchronization Error

Figure 3. No-load speed regulation experiment of the proposed method

It can be seen from Fig. 5 that under the multi-strategy improved cross-coupling control, the dynamic drop of the dual-motor speed is only 5 r/min after the sudden load application, the minimum speed change is reduced to 1 r/min, the speed quickly recovers to the synchronous state with a recovery time of about 0.05 s, the synchronization error is always maintained in a small range, and the influence of load disturbance on the system synchronization performance is extremely small.

In summary, under normal operating conditions, compared with the traditional cross-coupling control, the multi-strategy improved cross-coupling control method shortens the speed recovery time by 28% under the sudden load condition, reduces the speed fluctuation range by more than 90%, has higher synchronization error control precision, and the system robustness is significantly enhanced.

4. Conclusion

Based on the research and experimental simulation verification of this paper, the conclusions are as follows:

(1) Aiming at the problems of strong coupling, nonlinearity and time-varying disturbance of the dual PMSM system of mining electric locomotives, the proposed multi-strategy improved prescribed performance sliding mode cross-coupling control strategy can constrain the convergence rate and steady-state precision of the synchronization error through the prescribed performance function, and significantly improve the anti-disturbance capability of the system.

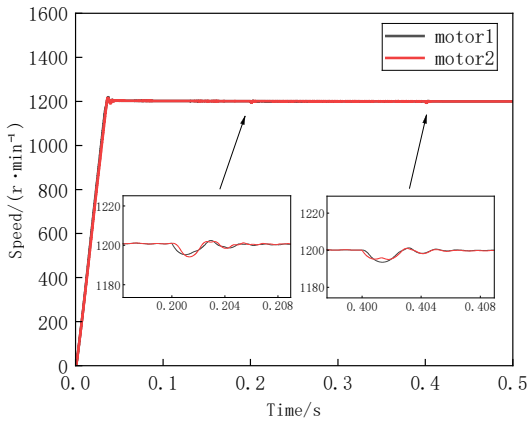

a) Output Speed

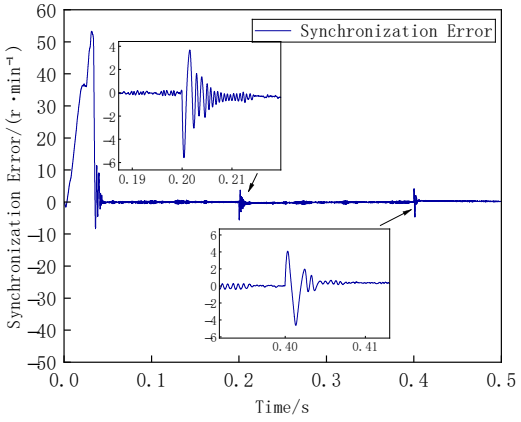

b) Synchronization Error

Figure 4. Load mutation experiment of traditional method

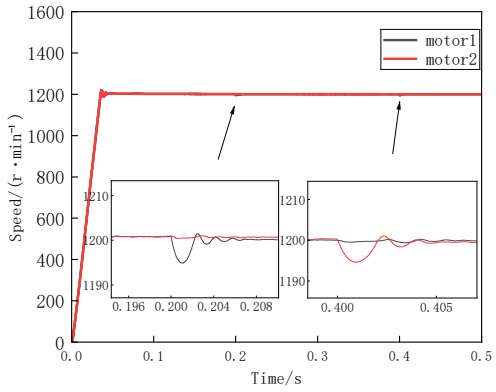

a) Output Speed

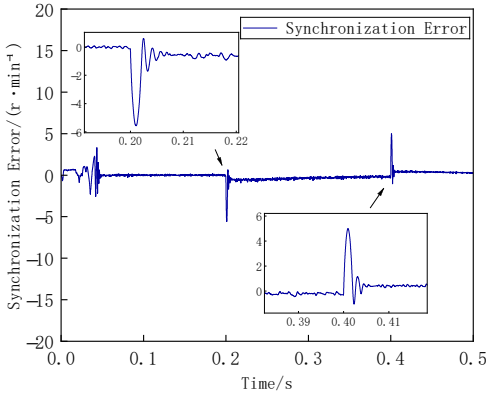

b) Synchronization Error

Figure 5. Load mutation experiment of the proposed method

(2) The no-load speed regulation simulation results show that this strategy reduces the adjustment time by 25% compared with the traditional cross-coupling control, controls the overshoot within 2%, has no oscillation in the transient process, and has better tracking performance.

(3) The sudden load simulation results show that this strategy shortens the speed recovery time by 28% compared with the traditional method, reduces the speed fluctuation range by more than 90%, the synchronization error is always kept in a small range, and the robustness is significantly enhanced.

References

[1] S. Ren, X. Jiao, D. Zheng, Y. Zhang, H. Xie, and R. Zhang: "Impact of Carbon Neutrality Goals on China's Coal Industry: Mechanisms and Evidence," Energies, Vol.18, pp.1672 (2025).

[2] Y. Hou, S. Xi, H. Li, Y. Fan, F. Li, and Q. Wen: "The Development of Circular Economy in China's Coal Industry: Facing Challenges of Inefficiency in the Waste Recycling Process," Sustainability, Vol.17, pp.8147 (2025).

[3] Z. J. Jin and C. Zhang: "On China's Energy Transition Pathway Towards Carbon Neutrality," Acta Scientiarum Naturalium Universitatis Pekinensis, Vol.60, pp.767–774 (2024).

[4] H. P. Xie, et al.: "Development opportunities of the coal industry towards the goal of carbon neutrality," Journal of China Coal Society, Vol.46, pp.2197–2211 (2021).

[5] Y. Gao, Y. Wang, G. Q. Wang, Y. S. Wang, and H. P. Liu: "Exploring on the construction paths to green mine in coal enterprises towards the goal of carbon peak and carbon neutrality," China Coal, Vol.48, pp.16–20 (2022).

[6] R. Huang, H. Cheng, and H. Zheng: "Study on master-slave control strategy of lower extremity exoskeleton robot," Proceeding of the 11th World Congress on Intelligent Control and Automation, Vol.00, pp.985–991 (2014).

[7] J. Shen, X. Wang, Z. Zhang, S. Ren, and D. Ma: "Research on the Application of Dual Three-Phase PMSM in Renewable Energy System," ICEMS, Vol.00, pp.3475–3479 (2023).

[8] J. Zhao, T. Cai, M. Xiong, and C. Yang: "Reinforcement Learning and Singular Perturbation-Based Optimal Speed Synchronous Control of a Flexible Coupling Dual-PMSM System," IEEE Trans. Ind. Informat., Vol.21, pp.9757–9765 (2025).

[9] N. Szlązak, M. Korzec, and J. Cheng: "Using Battery-Powered Suspended Monorails in Underground Hard Coal Mines to Improve Working Conditions in the Roadway," Energies, Vol.15, pp.7527 (2022).

[10] A. Cordeiro, J. F. M. Manuel, and V. F. Pires: "Performance of synchronized master-slave closed-loop control of AC electric drives using real time motion over ethernet (RTMoE)," Mechatronics, Vol.69, pp.102400 (2020).

[11] M. Guan, C. Qu, J. Lv, and L. Yang: "A novel RBF neural network–based sliding mode controller for a master–slave motor coordinated drive system," The International Journal of Advanced Manufacturing Technology, Vol.133, pp.4907–4921 (2024).

[12] O.-S. Kwon, S. H. Choe, and H. Heo: "A study on the dual-servo system using improved cross-coupling control method," International Conference on Environment and Electrical Engineering, Vol.00, pp.1–4 (2011).

[13] Z. Huang, Y. Li, G. Song, and X. Zhang: "Speed and Phase Adjacent Cross-Coupling Synchronous Control of Multi-Exciters in Vibration System Considering Material Influence," IEEE Access, Vol.7, pp.63204–63216 (2019).

[14] G. Han, Z. Lu, J. Hong, and M. Wu: "Speed Synchronization Control of Dual-SRM Drive With ISMC-Based Cross-Coupling Control Strategy," IEEE Trans. Transp. Electrific., Vol.9, pp.2524–2534 (2023).

[15] P. Fu, J. Pan, C. Wang, and R. Huang: "Research on coordinated control of multi-PMSLM based on sliding mode variable structure deviation coupling algorithm," ICEMS, Vol.00, pp.1–5 (2019).

[16] Z. Zhou, J. Wang, and S. Zhang: "Speed Synchronization Control Strategy of Dual-Motor System With Explicit Model Predictive Control," IEEE J. Emerg. Sel. Topics Power Electron., Vol.12, pp.2787–2798 (2024).

[17] B. Wang, M. Iwasaki, and J. Yu: "Command Filtered Adaptive Backstepping Control for Dual-Motor Servo Systems With Torque Disturbance and Uncertainties," IEEE Trans. Ind. Electron., Vol.69, pp.1773–1781 (2022).

[18] T.-I. Yeam and D.-C. Lee: "Design of Sliding-Mode Speed Controller With Active Damping Control for Single-Inverter Dual-PMSM Drive Systems," IEEE Trans. Power Electron., Vol.36, pp.5794–5801 (2021).

[19] C. Zhu, Q. Tu, C. Jiang, and M. Pan: "A Cross Coupling Control Strategy for Dual-Motor Speed Synchronous System Based on Second Order Global Fast Terminal Sliding Mode Control," IEEE Access, Vol.8, pp.217967–217976 (2020).

[20] F. Bian and Y.-R. Chien: "PMSM Speed Control Based on Improved Adaptive Fractional-Order Sliding Mode Control," Symmetry, Vol.17, pp.736 (2025).

[21] L. Liu, S. Ding, and S. Li: "Overview of high-order sliding mode control theory," Control Theory & Applications, Vol.39, pp.2193–2201 (2022).

[22] V. P. Tran, M. A. Mabrok, S. G. Anavatti, and M. A. Garratt: "Robust Adaptive Fuzzy Control for Second-Order Euler–Lagrange Systems With Uncertainties and Disturbances via

Nonlinear Negative-Imaginary Systems Theory," IEEE Trans. Cybern., Vol.54, pp.5102–5114 (2024).

[23] S. C. Tong, X. Min, and Y. X. Li: "Observer-Based Adaptive Fuzzy Tracking Control for Strict-Feedback Nonlinear Systems With Unknown Control Gain Functions," IEEE Trans. Cybern., Vol.50, pp.3903–3913 (2020).

[24] X. D. Wang and H. H. Shao: "Theory of RBF neural network and its application in control," Inf. Control, Vol.00, pp.1–13 (1997).

[25] M. K. Bao and Y. Z. Zhou: "Variable parameter displacement and speed parallel control of permanent magnet synchronous linear motor based on composite neural network reconstructed object," Trans. China Electrotech. Soc., Vol.39, pp.2470–2484 (2024).

[26] J. Wang: "Research on multi-motor coordinated control system of pure electric road-rail vehicle," (Ph.D. Thesis, Beijing Univ. Civil Eng. Archit., Beijing), Vol.00, pp.000-000 (2020).

[27] L. Zhang, J. S. Bao, and J. W. Hao: "Fuzzy active disturbance rejection deviation coupling multi-motor control strategy for permanent magnet direct drive belt conveyor," China Mech. Eng., Vol.35, pp.2071–2081 (2024).

[28] Q. Geng, L. Li, and Z. Q. Zhou: "Anti-disturbance speed synchronization control of dual permanent magnet motor system," Proc. CSEE, Vol.41, pp.6787–6796 (2021).

[29] C. L. Xia, L. Li, and X. Gu: "Speed synchronization control of dual permanent magnet motor system," Trans. China Electrotech. Soc., Vol.32, pp.1–8 (2017).

[30] E. L. Kang and J. Chen: "Improved sliding mode sensorless control of permanent magnet synchronous motor," Electr. Mach. Control, Vol.26, pp.88–97 (2022).